

Figure 8. Plot of  $\ln(k_{nr} + k_{dd})$  vs.  $E_{em}$  for  $\text{Ru}(\text{bpy})_{3-N}(\text{DMB})_N^{2+}$  complexes ( $N = 0-3$ ).

principally controlled by these nonradiative processes.

Meyer and co-workers have shown that the excited-state decay characteristics of these types of complexes can be adequately interpreted in terms of the energy gap law formalism,<sup>19,41-45</sup> that is, a plot of  $\ln k_{nr}$  vs. the emission energy is expected to be linear. In fact, these workers have recently reported results for several series of mixed-ligand complexes of Ru(II) containing the ligands 2,2'-bipyridine, 2,2'-bipyrazine (bpyz), and 2,2'-bipyrimidine (bpy). For the series  $\text{Ru}(\text{bpy})_{3-N}(\text{bpyz})_N^{2+}$ , plots of  $\ln k_{nr}$  vs.  $E_{em}$  were linear for  $N = 1, 2$ , and 3, but the point corresponding to  $\text{Ru}(\text{bpy})_3^{2+}$  was well removed from the line. Similar behavior was observed for the bpy/bpy series.<sup>45</sup> As Meyer and co-workers have emphasized, the observation of linearity of such plots depends on the validity of certain underlying assumptions, the most important of which, in the context of the present work, is that the members of the series possess a common lumiphore.<sup>19,41-45</sup> Thus, their results strongly imply that the excited state which dominates the decay properties is centered on a bpyz or bpy rather than a bpy ligand. This is consistent with the fact that the  $\pi^*$  levels of bpyz and bpy are lower than that of bpy. In order to carry

out a comparable analysis for the bpy/DMB series, it would be necessary to determine the values for  $k_{dd}$  via temperature-dependent lifetime measurements. However, provided that the relative contribution of  $k_{dd}$  to the  $(k_{nr} + k_{dd})$  sum varies smoothly through the series, plots of  $\ln(k_{nr} + k_{dd})$  vs.  $E_{em}$  may be expected to exhibit linearity. The expectation that  $k_{dd}$  should vary smoothly through the series (at least for  $\text{Ru}(\text{bpy})_{3-N}(\text{DMB})_N^{2+}$ ; where  $N = 0, 1$ , and 2) is based on the following considerations.

The value of  $k_{dd}$  is expected to decrease as  $\Delta E$  (Figure 7) increases. The energy of the  $d\pi$  orbitals (and presumably also the  $d\sigma^*$ ) have been shown to vary smoothly in other series of mixed-ligand complexes wherein the  $\text{Ru}(3+/2+)$  potentials were measured.<sup>28</sup> In the present series, the energy of  $d\sigma^*$  should thus increase smoothly as bpy is replaced by DMB. On the other hand, the  $\pi^*$  orbitals are ligand-localized and retain their relative energies in the mixed-ligand complexes.<sup>28</sup> In this series, the  $\pi^*$ -(DMB) orbitals are higher in energy than the  $\pi^*$ -(bpy) orbitals by  $\sim 800 \text{ cm}^{-1}$  based on the potentials given in Table III ( $1 \text{ eV} = 8065 \text{ cm}^{-1}$ ).

A plot of  $\ln(k_{nr} + k_{dd})$  vs.  $E_{em}$  for the present series of complexes is shown in Figure 8. The observation of linear behavior for the complexes corresponding to  $N = 0, 1$ , and 2 demonstrates that  $k_{dd}$  can be expressed as a constant fraction of  $k_{nr}$  and, most importantly, that these data are consistent with the  $\text{TR}^3$  data inasmuch as a common lumiphore (i.e., the  $(\text{Ru}^{\text{III}}(\text{bpy}^-))$  fragment is implicated).

The results presented here indicate that for a series of poly(pyridine) complexes, involving even a relatively mild chemical modification, the mixed-ligand complexes,  $\text{Ru}(\text{bpy})_2(\text{DMB})^{2+}$  and  $\text{Ru}(\text{bpy})(\text{DMB})_2^{2+}$ , possess isolated MLCT excited states with apparently insignificant interligand electronic coupling. The most obvious manifestation of such behavior is the observation of selective population of the lowest lying  $^3\text{MLCT}$  state. Furthermore, it has been shown that  $\text{TR}^3$  spectroscopy provides an especially effective and convenient method for the detection of this selectivity.

**Acknowledgment.** We thank Prof. T. Spiro of Princeton University and Prof. M. Barkley of Louisiana State University for use of equipment and facilities and Profs. Laren Tolbert (University of Kentucky), Paul Stein (Duqueene University), and Dennis Strommen (Carthage College) for very helpful comments. During part of this work, S.F.M. was supported by a University of Kentucky Graduate School Fellowship.

**Registry No.**  $\text{Ru}(\text{bpy})_3^{2+}$ , 15158-62-0;  $\text{Ru}(\text{bpy})_2(4,4'\text{-DMB})^{2+}$ , 70281-18-4;  $\text{Ru}(\text{bpy})(4,4'\text{-DMB})_2^{2+}$ , 97135-47-2;  $\text{Ru}(4,4'\text{-DMB})_3^{2+}$ , 32881-03-1.

- (41) Caspar, J. V.; Meyer, T. J. *J. Am. Chem. Soc.* **1983**, *105*, 5583-5590.  
 (42) Caspar, J. V.; Meyer, T. J. *Inorg. Chem.* **1983**, *22*, 2444-2453.  
 (43) Kober, E. M.; Sullivan, B. P.; Dressick, W. J.; Caspar, J. V.; Meyer, T. J. *J. Am. Chem. Soc.* **1980**, *102*, 7383-7385.  
 (44) Caspar, J. V.; Meyer, T. J. *J. Phys. Chem.* **1983**, *87*, 952-957.  
 (45) Allen, G. H.; White, R. P.; Rillema, D. P.; Meyer, T. J. *J. Am. Chem. Soc.* **1984**, *106*, 2613-2620.

## Infrared Intensities: Cyclohexane. A Molecular Force Field and Dipole Moment Derivatives

Kenneth B. Wiberg,\* Valerie A. Walters, and William P. Dailey

Contribution from the Department of Chemistry, Yale University, New Haven, Connecticut 06511. Received March 4, 1985

**Abstract:** A force field derived from an ab initio molecular orbital procedure by using the 4-31G basis set was taken as the starting point for a normal coordinate analysis. The calculated F matrix was adjusted to fit the experimental vibrational frequencies and led to a root-mean-square error of  $10 \text{ cm}^{-1}$ . The intensities of the vibrational bands of cyclohexane and cyclohexane- $d_{12}$  were measured and were transformed into dipole moment derivatives. The signs of  $\partial\mu/\partial S$  are discussed in terms of a model we have developed for their interpretation.

Cyclohexane plays a special role in the study of cycloalkanes and related compounds. It is usually taken as the "unstrained"

model against which other compounds are compared, and force constants derived from cyclohexane have been used as the "normal"

Table I. Raman Spectrum of Cyclohexane ( $\text{cm}^{-1}$ )

mode		$d_0$		$d_{12}$	
		gas	liquid	gas	liquid
$A_{1g}$	1	2950	2938	2162	2150
	2	2864	2854	2089	2081
	3	1472	1466	1123	1119
	4	1161	1158	1016	1013
	5	801	801	722	723
	6		382	<i>a</i>	298
$E_g$	9	2935	2924	2203	2196
	10	2877	2867	2113	2102
	11	1450	1445	<i>a</i>	1213
	12	<i>a</i>	1347	<i>a</i>	1074
	13	1270	1266	940	937
	14	1032	1028	801	796
	15	<i>a</i>	786	<i>a</i>	635
	16	<i>a</i>	427	<i>a</i>	375

<sup>a</sup>The band was too weak to be observed in the gas-phase spectrum.

force constants for some molecular mechanics calculations.<sup>1</sup> Thus, it is important to understand the intramolecular interactions in cyclohexane. Molecular spectroscopy provides the only experimental tool for studying these interactions, and we have previously reported a detailed study of the vibrational spectra of cyclohexane and three of its deuterium-labeled derivatives.<sup>2-4</sup> Earlier studies of the infrared and Raman spectra of cyclohexane have been reviewed.<sup>2</sup>

The determination of a vibrational force field for a molecule as large as cyclohexane from experimental vibrational frequencies is fraught with difficulties. The E blocks, for example, require 36 independent elements of the F matrix. It is not readily possible to obtain this large a number of independent data, and thus in a conventional normal coordinate analysis one must make assumptions about some of the off-diagonal elements of the matrix. In our earlier study, the molecular vibrations of cyclohexane, cyclohexane- $d_{12}$ , cyclohexane-1,1,4,4- $d_4$ , and cyclohexane-2,2,3,3,5,5,6,6- $d_8$  were assigned and a normal coordinate analysis of these data was presented.<sup>2-4</sup> However, for the reason given above, it is quite possible that the derived force field is partially in error. Therefore, we have reinvestigated the force field and also have obtained information on the intensities of the infrared bands in order to derive the dipole moment derivatives. They were of interest in connection with the model we have developed for interpreting these derivatives.<sup>5</sup>

One difficulty with the previously available experimental data should first be noted. Whereas the infrared spectra have generally been obtained in the gas phase, the Raman spectra of cyclohexane have always been obtained in the liquid phase. Since cyclohexane has a center of symmetry, there is no overlap between the infrared and Raman spectra. As a result, there was no way in which the gas-phase Raman frequencies could be estimated. Therefore, we have determined the gas-phase Raman spectra of cyclohexane and cyclohexane- $d_{12}$  (Figure 1), giving the data shown in Table I. The  $A_{1g}$  bands were easily recognized because they are polarized and have intense Q branches. The  $E_g$  bands have a variety of band shapes which depend on the Coriolis coupling constants,  $\zeta$ . One of the  $E_g$  CH stretching bands was easily located at  $2935 \text{ cm}^{-1}$ . The other band probably corresponds to one of the weak bands at  $2877$  and  $2897 \text{ cm}^{-1}$ . The ab initio calculations presented below as well as preliminary normal coordinate calculations suggested that  $2877 \text{ cm}^{-1}$  was the more satisfactory value. With cyclohexane- $d_{12}$ , all of the four CD stretching bands could be observed. A number of the other  $E_g$  bands of both molecules also could be observed. It can be seen that the CH and CD bands suffer a relatively large shift on going from the gas to the liquid phase,

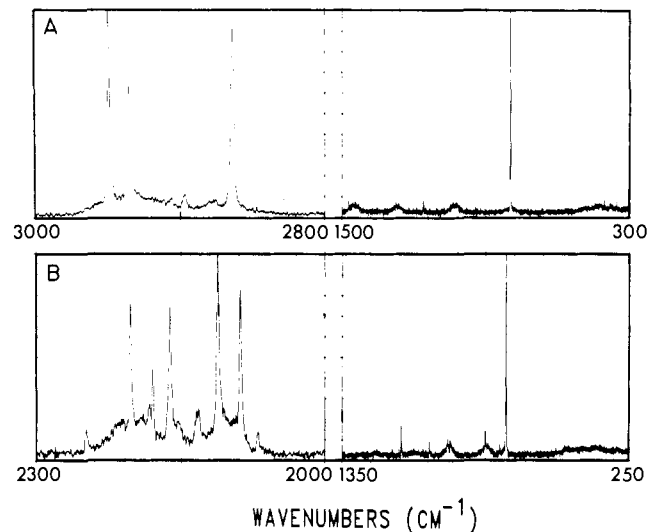


Figure 1. Gas-phase Raman spectra of cyclohexane (A) and cyclohexane- $d_{12}$  (B).

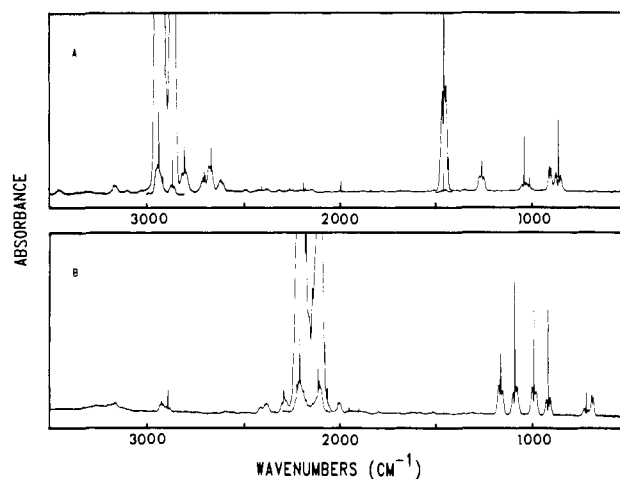


Figure 2. Infrared spectra of cyclohexane (A) and cyclohexane- $d_{12}$  (B). In A, the pressures were 63 torr (upper) and 1.4 torr (lower), and in B the pressures were 60 torr (upper) and 4.5 torr (lower). Path length = 7.3 cm.

whereas the bands below  $1600 \text{ cm}^{-1}$  show only small shifts. Thus, for the lower frequency weak bands in the Raman spectrum which cannot be seen in the gas phase, it was satisfactory to use the liquid-phase values.

The infrared spectra of cyclohexane and cyclohexane- $d_{12}$  also were determined at a high resolution ( $0.06 \text{ cm}^{-1}$ ), and the band positions given in the tables are derived from these spectra. Here, again, there was difficulty in locating the CH and CD stretching bands (Figure 2). Many of the bands in these regions result from overtones and combination bands and are probably affected by Fermi resonance which causes them to borrow intensity from the fundamental bands. In cyclohexane there are two intense CH bands along with the many weaker ones. Since the calculations suggested that each of the two  $A_{2u}$  bands should be rather close to one of the two  $E_u$  bands, it was assumed that the two sets of bands were coincident. The same is true for the CD bands of cyclohexane- $d_{12}$ . The previous assignments for all of the other bands appear to be satisfactory.

It now appears that the more satisfactory way in which to derive a molecular force field is to first calculate the forces by using an ab initio molecular orbital procedure.<sup>6</sup> This gives both the F matrix and dipole moment derivatives from which the infrared intensities may be estimated. The F matrix was calculated in

(1) Cf.: Burkert, U.; Allinger, N. L. "Molecular Mechanics"; American Chemical Society: Washington, D.C., 1982; ACS Monograph 177, p 90ff.

(2) Wiberg, K. B.; Shrake, A. *Spectrochim. Acta* 1971, 27A, 1139.

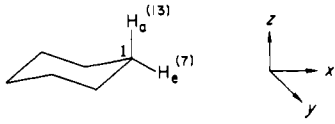
(3) Wiberg, K. B.; Shrake, A. *Spectrochim. Acta* 1973, 29A, 567.

(4) Wiberg, K. B.; Shrake, A. *Spectrochim. Acta* 1973, 29A, 583.

(5) Wiberg, K. B.; Wendoloski, J. J., *J. Phys. Chem.* 1984, 88, 586.

(6) Pulay, P. In "The Force Concept in Chemistry"; Deb, B. M., Ed.; Van Nostrand: New York, 1981.

Table II. Calculated Geometry for Cyclohexane



parameter	calcd	obsd <sup>a</sup>	used <sup>b</sup>
$r(\text{C}-\text{C})$	1.534	$1.536 \pm 0.002$	1.536
$r(\text{C}-\text{H}_e)$	1.086	$1.116 \pm 0.004$	1.106
$r(\text{C}-\text{H}_a)$	1.088	(av)	
$\angle\text{C}-\text{C}-\text{C}$	111.37	$111.4 \pm 0.2$	111.4
$\angle\text{C}-\text{C}-\text{H}_e$	110.08		110.1
$\angle\text{C}-\text{C}-\text{H}_a$	109.13		109.1
$\angle\text{H}-\text{C}-\text{H}$	106.94	$107.5 \pm 1.5$	107.0
$\tau(\text{CCCC})$	55.03	$54.9 \pm 0.4$	54.9

<sup>a</sup>Bastiansen, O.; Fernholt L.; Seip, H. M. *J. Mol. Struct.* **1973**, *18*, 163. Ewbank, J. D.; Kirsch, G.; Schafer, L. *Ibid.* **1976**, *31*, 39. Units: Å and degrees. <sup>b</sup>Geometry used in calculating the G matrix used in the normal coordinate calculations. The observed CH bond length is unusually large for an alkane whereas the calculated length is normal. The value used is the average where the observed value was given a weighting factor of 2.

Cartesian coordinates with the 4-31G basis set<sup>7</sup> and the theoretically derived minimum energy geometry (Table II). This basis set has been found to be satisfactory for force constant estimations.<sup>8</sup> The vibrational frequencies derived from the F matrix along with the calculated intensities are listed in Table III.

It may appear strange to compare harmonic calculated frequencies obtained at the theoretical geometry with anharmonic observed frequencies which are based on the experimental geometry. However, it has been found that using this procedure, the calculated and observed frequencies stand in essentially constant ratio.<sup>5,8</sup> Apparently, the combined effects of anharmonicity, neglect of electron correlation, and use of the theoretical geometry combine to yield a simple correlation between the two sets of frequencies. We have found with other molecules that the C-H stretching frequencies should be scaled by the factor  $0.91 \pm 0.1$  and that the other frequencies should be scaled by  $0.88 \pm 0.02$ .<sup>5,9-11</sup> Similar scaling factors have been found by other investigators.<sup>12</sup> The scaled frequencies are compared with the observed frequencies for cyclohexane and cyclohexane- $d_{12}$  in Table III, and a good agreement is found, with a root-mean-square error of only  $22 \text{ cm}^{-1}$ . In the case of modes having frequencies below  $2000 \text{ cm}^{-1}$ , all of the scaled values which differ from the experimental frequencies by more than  $25 \text{ cm}^{-1}$  are lower than the experimental values and, as will be shown below, involve a major contribution from C-C bond stretching. If a larger scaling factor had been used (such as that for C-H bond stretching), the agreement would have been significantly better.

One potential problem in any such comparison, and also with normal coordinate analyses, is that the modes corresponding to the several vibrations may not properly come in a simple numerical order. Thus for the  $E_u$  block of cyclohexane, it is possible that one vibrational mode might correspond to the  $1252 \text{ cm}^{-1}$  calculated frequency and the  $1346 \text{ cm}^{-1}$  observed frequency and that another corresponds to  $1356 \text{ cm}^{-1}$  calculated and  $1260 \text{ cm}^{-1}$  observed. Just as with NMR spectroscopy,<sup>13</sup> the only way to guard against such cross-assignments is to examine the intensities. The qualitative

observed intensities are compared with the calculated intensities in Table III, and here it is seen that the simple correlation is satisfactory. The results presented in the table strongly suggest that the vibrational assignment is correct and that the calculated force field, after being scaled, would give a good representation of the true force field.

We wish to obtain a "best fit" force field by adjusting the calculated F matrix to give vibrational frequencies which agree with the observed frequencies as well as possible. We do not have experimental corrections for anharmonicity, and we are hesitant to make simple assumptions about the vibrational modes for a molecule of this size. Therefore, we have adjusted the F matrix to fit the observed anharmonic frequencies.

The ab initio calculated F matrix with respect to Cartesian coordinates was converted to that corresponding to internal coordinates with the inverse of the  $3n \times 3n$  B matrix which had been augmented by the translational and rotational terms required to satisfy the Eckart conditions.<sup>14</sup> The set of internal coordinates consisted of the six C-C bonds, the twelve C-H bonds, the six C-C-C bond angles, and the twenty-four C-C-H bond angles. It may be noted that neither the H-C-H angles nor the torsional angles were included. The former are never needed at methylene groups because the geometry is completely defined by using only five of the six possible angles. It is convenient to use the C-C-C angle and the four C-C-H angles at each  $\text{CH}_2$  group. In the case of cyclohexane, the torsional angles are related to the C-C-C angles, and the latter were chosen. The conversion from force constants in Cartesian coordinates to those in internal coordinates can be effected in a unique fashion only if the internal coordinates contain no redundancies.

There is strong coupling between some of the diagonal and off-diagonal elements of the matrix, and therefore some constraint must be placed on the adjustment. In the normal coordinate calculations, six independent scaling factors were used, one for each of the six different types of internal coordinates (i.e., C-C stretch, axial C-H stretch, equatorial C-H stretch, C-C-C bend, axial C-C-H bend, and equatorial C-C-H bend). We have adopted the suggestion of Pulay et al.<sup>15</sup> that the scaling factors for the interaction constants be set as the geometric mean of those for the corresponding internal coordinates. In the fitting procedure, the gas-phase frequencies were given a weighting factor of 2 whereas the liquid-phase frequencies were given a weighting factor of 1. In the calculations, the data for cyclohexane, cyclohexane- $d_{12}$ , and the CH stretching frequencies observed for cyclohexane- $d_{11}$  (axial CH  $2891 \text{ cm}^{-1}$ , equatorial CH  $2923 \text{ cm}^{-1}$ )<sup>16</sup> were used. The latter were included because of the difficulties in assigning the CH stretching bands in the infrared spectrum. The symmetry coordinates used for cyclohexane are given in Table IV. The resulting "best fit" scaling factors led to a root-mean-square error of  $10.2 \text{ cm}^{-1}$ . The calculated vibrational frequencies are compared with the observed frequencies in Table V.

The constants derived above were used to calculate the vibrational frequencies for the partially labeled cyclohexanes having  $C_{2h}$  symmetry. Their symmetry coordinates are given in Table VI. The previous assignments were well reproduced in most cases, but a few bands had differences of  $25\text{--}55 \text{ cm}^{-1}$ . The vibrational assignments for these bands were reexamined by making use of the intensities derived from the L matrices obtained in fitting the experimental data and the polar tensors obtained from the ab initio

(7) Ditchfield, R.; Hehre, W. J.; Pople, J. A. *J. Chem. Phys.* **1971**, *54*, 724.

(8) Pople, J. A.; Schlegel, H. B.; Krishnan, R.; DeFrees, D. J.; Binkley, J. S.; Frisch, M. J.; Whiteside, R. A.; Hout, R. F.; Hehre, W. J. *Int. J. Quantum Chem., Quantum Chem. Symp.* **1981**, *15*, 269.

(9) Wiberg, K. B.; Walters, V.; Colson, S. D. *J. Phys. Chem.* **1984**, *88*, 4723.

(10) Wiberg, K. B.; Dempsey, R. C.; Wendoloski, J. J. *J. Phys. Chem.* **1984**, *88*, 5596.

(11) Wiberg, K. B.; Walters, V. A.; Wong, K.; Colson, S. D. *J. Phys. Chem.* **1984**, *88*.

(12) Blom, C. E.; Slingerland, P. J.; Altona, C. *Mol. Phys.* **1976**, *31*, 1359. Cf. ref 8 and 15.

(13) Pople, J. A.; Schneider, W. G.; Bernstein, H. J. "High-resolution Nuclear Magnetic Resonance"; McGraw-Hill, NY, 1959.

(14) Eckart, C. *Phys. Rev.* **1935**, *47*, 552. Sayvetz, A. *J. Chem. Phys.* **1939**, *7*, 383.

(15) Pulay, P.; Fogarasi, F.; Ponder, G.; Boggs, J. E.; Vargha, A. *J. Am. Chem. Soc.* **1983**, *105*, 7037.

(16) Wong, J. S.; MacPhail, R. A.; Moore, C. B.; Strauss, H. L. *J. Phys. Chem.* **1982**, *86*, 1478.

(17) Dickson, A. D.; Mills, I. M.; Crawford, B., Jr. *J. Chem. Phys.* **1957**, *27*, 445.

(18) Wilson, E. B., Jr.; Wells, A. J. *J. Chem. Phys.* **1946**, *14*, 578. Penner, S. S.; Weber, D. *Ibid.*, **1951**, *19*, 807.

(19) Dupuis, M.; Spangler, D.; Wendoloski, J. J. National Resource for Computation in Chemistry Program QG01, 1980.

(20) Schachtschneider, J. H. Technical Report 231-64, Shell Development Co., 1966.

(21) Dempsey, R. C. Ph.D. Thesis, Yale University, 1983.

Table III. Calculated Vibrational Frequencies for Cyclohexane ( $\text{cm}^{-1}$ )

mode	cyclohexane- $d_0^e$						cyclohexane- $d_{12}^f$					
	calcd	scaled <sup>a</sup>	obsd	int <sup>b</sup>		calcd	scaled	obsd	int			
				calcd	obsd <sup>c</sup>				calcd	obsd		
A <sub>1g</sub>	1	3190	2935	2950		2361	2172	2162				
	2	3136	2885	2864		2298	2114	2089				
	3	1672	1472	1472		1255	1104	1123				
	4	1315	1157	1161		1139	1002	1016				
	5	846	744	801		767	675	722				
	6	402	354	382 <sup>d</sup>		315	277	298 <sup>d</sup>				
A <sub>2g</sub>	7	1522	1339			1202	1058					
	8	1196	1053			847	745					
E <sub>g</sub>	9	3186	2931	2935		2365	2176	2203				
	10	3137	2886	2877		2283	2100	2113				
	11	1652	1454	1450		1325	1166	1213 <sup>d</sup>				
	12	1520	1337	1347 <sup>d</sup>		1220	1073	1074 <sup>d</sup>				
	13	1420	1250	1270		1049	923	940				
	14	1124	989	1032		883	771	801				
	15	882	776	786 <sup>d</sup>		713	627	635 <sup>d</sup>				
	16	471	414	427 <sup>d</sup>		414	364	375 <sup>d</sup>				
A <sub>1u</sub>	17	1510	1328			1296	1140					
	18	1262	1110			969	853					
	19	1176	1035			892	785					
A <sub>2u</sub>	20	3199	2943	2933	194.8	vs	2376	2185	2206	93.8	vs	
	21	3137	2886	2862	70.7	vs	2285	2102	2111	43.8	vs	
	22	1664	1464	1457	17.0	s	1238	1089	1092	6.9	s	
	23	1153	1014	1039	2.9	w	1014	892	917	4.7	m	
	24	580	510	520	0.7	vw	440	387	394	0.5	vw	
E <sub>u</sub>	25	3183	2928	2933	310.4	vs	2357	2168	2206	96.4	vs	
	26	3133	2882	2862	60.8	vs	2289	2083	2111	86.2	vs	
	28	1654	1455	1457	9.0	s	1287	1132	1164	5.2	s	
	28	1541	1356	1346	0.2	vw	1216	1070	1070	1.0	vw	
	29	1423	1252	1260	3.6	m	1110	976	991	6.4	s	
	30	1024	901	906	7.4	m	780	686	720	0.0	w	
	31	919	809	863	3.8	m	773	680	687	6.2	m	
	32	247	218	241	0.0		200	176		0.0		

<sup>a</sup>Scaling factors: CH stretch, 0.92; others, 0.88. <sup>b</sup>km/mol. The intensities for the E<sub>u</sub> block include the degeneracy factor of 2. <sup>c</sup>Qualitative relative intensities. <sup>d</sup>Liquid-phase values. <sup>e</sup>rms error = 22  $\text{cm}^{-1}$ . <sup>f</sup>rms error = 22  $\text{cm}^{-1}$ .

calculation. With the  $d_4$  compound, it appeared that the 802- $\text{cm}^{-1}$  band should be assigned as  $\nu_{46}$  rather than  $\nu_{45}$  and that the weak band at 765  $\text{cm}^{-1}$  which is seen only in the liquid may be an artifact. In the case of the  $d_8$  compound, it appeared that the 927- $\text{cm}^{-1}$  band should be assigned as  $\nu_{31}$  rather than  $\nu_{32}$  and that the 1103- $\text{cm}^{-1}$  band should be assigned as  $\nu_{42}$  rather than  $\nu_{29}$ . With these changes, the root-mean-square error for  $d_4$  was 8.7  $\text{cm}^{-1}$  and that for  $d_8$  was 10.7  $\text{cm}^{-1}$ . A cycle of scaling factor adjustment which included the data for these compounds led to no significant change. The calculated and observed frequencies are compared in Table VII, and the scaling factors are given in Table VIII. As might be anticipated from the above discussion, the scaling factors for the stretching force constants were significantly larger than those for the bending constants. The values of the scaling factors are close to those observed with other molecules.

It is not practical to list the final force constant matrix in internal coordinates because of the larger number of off-diagonal elements. They may be presented with more compact and in a more useful form in terms of the symmetry coordinates (Table IX). The force constants for the stretching modes are similar to those obtained previously,<sup>4</sup> and those for the bending modes are different because redundant coordinates were included in the previous study. The main differences are found with the off-diagonal elements of the F matrix. Many of them are now found to be rather large (0.8 to 1.4  $\text{mdyn}/\text{\AA}$ ). This is particularly true with the bending coordinates (such as  $f_{4,5}$ ,  $f_{5,6}$ ,  $f_{13,14}$ ,  $f_{15,16}$ ,  $f_{22,23}$ ,  $f_{23,24}$ , and  $f_{28,29}$ ). The fact that the calculated ab initio force field was able to reproduce the observed vibrational frequencies with a root-mean-square error of only 22  $\text{cm}^{-1}$  by using just the two scaling factors which have been found to be appropriate for a variety of molecules as different as cyclopropene,<sup>10</sup> acetaldehyde,<sup>9</sup> and pyridine<sup>11</sup> strongly suggests that the large interaction constants

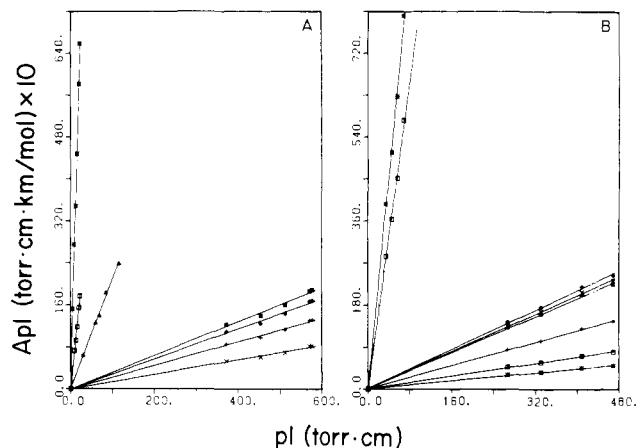


Figure 3. Beer's law plots for cyclohexane (A) and cyclohexane- $d_{12}$  (B).

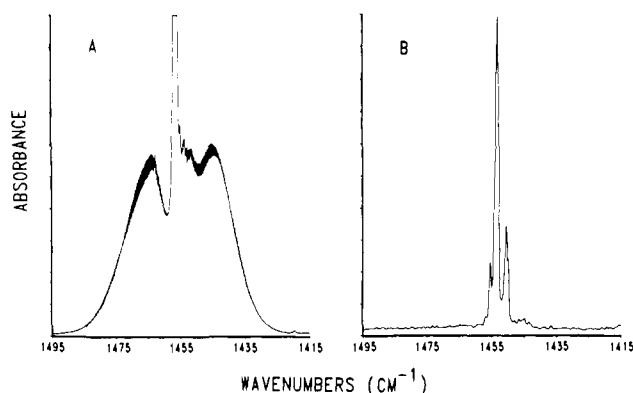
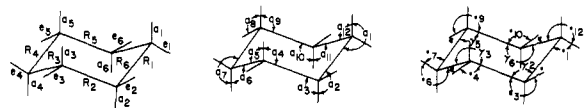
are appropriate for cyclohexane. It remains to determine their physical origin, and this will be studied in connection with current work on other related molecules.

It should be clear that it would not be possible to obtain satisfactory force fields for cyclohexane and related molecules without making use of ab initio calculated force constants as a starting point. Similarly, the following discussion of intensities would be impractical without the calculated polar tensors as a starting point. In the absence of such information, the sign problem which results from taking the square root of the observed intensities would be almost impossible to overcome.

With a vibrational force field in hand, we may now consider the band intensities. The infrared spectra of  $d_0$  and  $d_{12}$  are shown

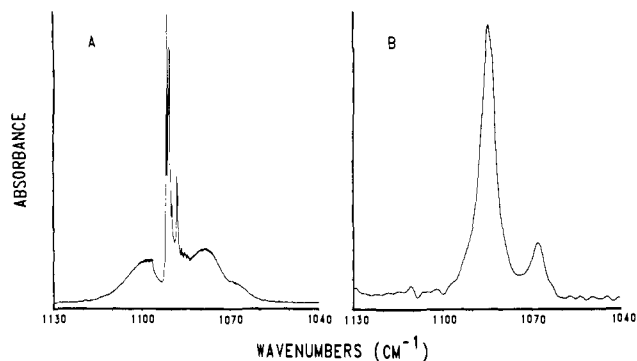
**Table IV.** Symmetry Coordinates for Cyclohexane,  $D_{3d}$ 

$A_{1g}$	$S_1 = R_1 + R_2 + R_3 + R_4 + R_5 + R_6$
	$S_2 = a_1 + a_2 + a_3 + a_4 + a_5 + a_6$
	$S_3 = e_1 + e_2 + e_3 + e_4 + e_5 + e_6$
	$S_4 = \gamma_1 + \gamma_2 + \gamma_3 + \gamma_4 + \gamma_5 + \gamma_6$
	$S_5 = \alpha_1 + \alpha_2 + \alpha_3 + \alpha_4 + \alpha_5 + \alpha_6 + \alpha_7 + \alpha_8 + \alpha_9 + \alpha_{10} + \alpha_{11} + \alpha_{12}$
	$S_6 = \epsilon_1 + \epsilon_2 + \epsilon_3 + \epsilon_4 + \epsilon_5 + \epsilon_6 + \epsilon_7 + \epsilon_8 + \epsilon_9 + \epsilon_{10} + \epsilon_{11} + \epsilon_{12}$
$A_{2g}$	$S_7 = \alpha_1 - \alpha_2 + \alpha_3 - \alpha_4 + \alpha_5 - \alpha_6 + \alpha_7 - \alpha_8 + \alpha_9 - \alpha_{10} + \alpha_{11} - \alpha_{12}$
	$S_8 = \epsilon_1 - \epsilon_2 + \epsilon_3 - \epsilon_4 + \epsilon_5 - \epsilon_6 + \epsilon_7 - \epsilon_8 + \epsilon_9 - \epsilon_{10} + \epsilon_{11} - \epsilon_{12}$
$E_g$	$S_9 = 2R_1 - R_2 - R_3 + 2R_4 - R_5 - R_6$
	$S_{10} = a_1 + a_2 - 2a_3 + a_4 + a_5 - 2a_6$
	$S_{11} = e_1 + e_2 - 2e_3 + e_4 + e_5 - 2e_6$
	$S_{12} = \gamma_1 + \gamma_2 - 2\gamma_3 + \gamma_4 + \gamma_5 - 2\gamma_6$
	$S_{13} = 2\alpha_1 + 2\alpha_2 - \alpha_3 - \alpha_4 - \alpha_5 - \alpha_6 + 2\alpha_7 + 2\alpha_8 - \alpha_9 - \alpha_{10} - \alpha_{11} - \alpha_{12}$
	$S_{14} = \alpha_3 - \alpha_4 - \alpha_5 + \alpha_6 + \alpha_9 - \alpha_{10} - \alpha_{11} + \alpha_{12}$
	$S_{15} = 2\epsilon_1 + 2\epsilon_2 - \epsilon_3 - \epsilon_4 - \epsilon_5 - \epsilon_6 + 2\epsilon_7 + 2\epsilon_8 - \epsilon_9 - \epsilon_{10} - \epsilon_{11} - \epsilon_{12}$
	$S_{16} = \epsilon_3 - \epsilon_4 - \epsilon_5 + \epsilon_6 + \epsilon_9 - \epsilon_{10} - \epsilon_{11} + \epsilon_{12}$
$A_{1u}$	$S_{17} = R_1 - R_2 + R_3 - R_4 + R_5 - R_6$
	$S_{18} = \alpha_1 + \alpha_2 - \alpha_3 - \alpha_4 + \alpha_5 + \alpha_6 - \alpha_7 - \alpha_8 + \alpha_9 + \alpha_{10} - \alpha_{11} - \alpha_{12}$
	$S_{19} = \epsilon_1 + \epsilon_2 - \epsilon_3 - \epsilon_4 + \epsilon_5 + \epsilon_6 - \epsilon_7 - \epsilon_8 + \epsilon_9 + \epsilon_{10} - \epsilon_{11} - \epsilon_{12}$
$A_{2u}$	$S_{20} = a_1 - a_2 + a_3 - a_4 + a_5 - a_6$
	$S_{21} = e_1 - e_2 + e_3 - e_4 + e_5 - e_6$
	$S_{22} = \gamma_1 - \gamma_2 + \gamma_3 - \gamma_4 + \gamma_5 - \gamma_6$
	$S_{23} = \alpha_1 - \alpha_2 - \alpha_3 + \alpha_4 + \alpha_5 - \alpha_6 - \alpha_7 + \alpha_8 + \alpha_9 - \alpha_{10} - \alpha_{11} + \alpha_{12}$
	$S_{24} = \epsilon_1 - \epsilon_2 - \epsilon_3 + \epsilon_4 + \epsilon_5 - \epsilon_6 - \epsilon_7 + \epsilon_8 + \epsilon_9 - \epsilon_{10} - \epsilon_{11} + \epsilon_{12}$
$E_u$	$S_{25} = 2R_1 + R_2 - R_3 - 2R_4 - R_5 + R_6$
	$S_{26} = a_1 + a_2 - a_4 - a_5$
	$S_{27} = e_1 + e_2 - e_4 - e_5$
	$S_{28} = \gamma_1 + \gamma_2 - \gamma_4 - \gamma_5$
	$S_{29} = 2\alpha_1 + 2\alpha_2 + \alpha_3 + \alpha_4 - \alpha_5 - \alpha_6 - 2\alpha_7 - 2\alpha_8 - \alpha_9 - \alpha_{10} + \alpha_{11} + \alpha_{12}$
	$S_{30} = \alpha_3 - \alpha_4 + \alpha_5 - \alpha_6 - \alpha_9 + \alpha_{10} - \alpha_{11} + \alpha_{12}$
	$S_{31} = 2\epsilon_1 + 2\epsilon_2 + \epsilon_3 + \epsilon_4 - \epsilon_5 - \epsilon_6 - 2\epsilon_7 - 2\epsilon_8 - \epsilon_9 - \epsilon_{10} + \epsilon_{11} + \epsilon_{12}$
	$S_{32} = \epsilon_3 - \epsilon_4 + \epsilon_5 - \epsilon_6 - \epsilon_9 + \epsilon_{10} - \epsilon_{11} + \epsilon_{12}$

**Figure 4.** Infrared spectrum of cyclohexane showing the overlapping bands  $\nu_{22}$  and  $\nu_{27}$ . The gas-phase spectrum is shown in A (63 torr, 7.3 cm, 0.06-cm<sup>-1</sup> resolution), and the argon matrix spectrum is shown in B (633:1 Ar:cyclohexane, 20 K, 0.5-cm<sup>-1</sup> resolution).

in Figure 2. These compounds are remarkable in the simplicity of their spectra and the relative lack of overlapping bands below 2000 cm<sup>-1</sup>. The intensities were measured by using pressure broadening (300 psi of nitrogen)<sup>17</sup> and a spectrometer resolution of 0.24 cm<sup>-1</sup>. Beer's law plots were linear (Figure 3) and gave the intensities shown in Table X.

In cyclohexane, the band at 1457 cm<sup>-1</sup> consists of  $\nu_{22}$  and  $\nu_{27}$ . They could be resolved in the matrix spectrum (Figure 4), and

**Figure 5.** Infrared spectrum of cyclohexane- $d_{12}$  showing the overlapping bands  $\nu_{22}$  and  $\nu_{28}$ . The gas-phase spectrum is shown in A (60 torr, 7.3 cm, 0.06-cm<sup>-1</sup> resolution), and the solution spectrum is shown in B (0.06 M, 2-cm<sup>-1</sup> resolution, 0.015-cm path length).

computer simulation of the band gave intensities of 2.7 km/mol for the unassigned high-frequency component, 13.5 for  $\nu_{22}$ , and 4.4 for  $\nu_{27}$ . In cyclohexane- $d_{12}$ , the band at  $\sim 1090$  cm<sup>-1</sup> consists of  $\nu_{22}$  and  $\nu_{28}$ . The two could easily be resolved in the solution spectrum (Figure 5), and computer simulation gave intensities of 4.43 km/mol for  $\nu_{22}$  and 0.84 km/mol for  $\nu_{28}$ .

The CH and CD stretching regions presented the greatest difficulty in assigning intensities. As indicated above, one finds overtones and combination bands along with the fundamentals, and there are probably examples of intensity perturbation due to Fermi resonance. One possible way in which to partition the total intensity among the overlapping modes is to make use of the calculated intensities. Although the latter are frequently somewhat too large for CH stretching modes, it is likely that the relative intensities would be more accurate. In cyclohexane, the ratio of the calculated intensities for  $\nu_{20} + \nu_{25}$  to  $\nu_{21} + \nu_{26}$  is 3.84 and the ratio of the observed intensities is 3.41. Similarly, with cyclohexane- $d_{12}$ , the ratio of the calculated intensities is 1.46 and the observed ratio is 1.44. The good agreement between these ratios suggests that this approach is useful. In this fashion, the intensities for cyclohexane were estimated to be the following:  $\nu_{20}$ , 109.1;  $\nu_{21}$ , 44.4;  $\nu_{25}$ , 173.9; and  $\nu_{26}$ , 38.2 km/mol. The corresponding intensities for cyclohexane- $d_{12}$  were 59.7, 28.3, 61.3, and 55.7 km/mol.

With these data in hand, it is possible to make use of the  $L^{-1}$  matrices derived from the normal coordinate analysis to transform  $\partial\mu/\partial Q$  to  $\partial\mu/\partial S$ . Here it was assumed that the signs obtained in the ab initio calculations were correct. Since the anharmonicity corrections are not known, the term  $\nu_i/\omega_i$  in the intensity expression was taken as unity. The values thus determined are given in Table XI, and it can be seen that the results for the two isotopic species are in agreement. The polarization of the  $\partial\mu/\partial S$  for the  $A_{2u}$  block is along the  $z$  axis, whereas that for the  $E_u$  block is rotated 30° from the  $x$  axis in the  $xy$  plane. The  $\partial\mu/\partial S$  for this block are given for a coordinate system rotated 30° from the original so that they can be given as single numbers.

In order to obtain data which might better determine the dipole moment derivative for the C-H stretching modes, the spectrum of cyclohexane- $d_{11}$  was examined. Here, one finds two CH stretching modes, one for the conformer with an equatorial CH and one for the conformer with an axial CH (Figure 6).<sup>16</sup> The total band intensity was measured and found to be 38.0 km/mol. This intensity is somewhat too large because the cyclohexane- $d_{11}$  (98%) contained about 20% cyclohexane- $d_{10}$ , and here both hydrogens would contribute to the intensity. The corrected intensity for the  $d_{11}$  compounds would then be 31.7 km/mol. The bands were sufficiently well separated that the overlap could easily be estimated (Figure 6). Assuming equal proportions of the two conformers, the intensities were the following: equatorial CH 36.4 km/mol; axial CH 27.0 km/mol.

The intensities for the infrared bands of all three compounds were calculated from the averaged polar tensors (Table XII) corresponding to the dipole moment derivatives given in Table XI. The results are compared with the observed intensities in

Table V. Results of Normal Coordinate Analysis ( $\text{cm}^{-1}$ )

mode	cyclohexane- $d_0^a$				cyclohexane- $d_{12}^b$		
	calcd	obsd	description	calcd	obsd	description	
$A_{1g}$	1	2950	2950	88 $S_3$ , 4 $S_1$	2180	2162	68 $S_3$ , 21 $S_2$
	2	2870	2864	93 $S_2$ , 4 $S_3$	2106	2089	67 $S_2$ , 23 $S_3$
	3	1470	1472	35 $S_5$ , 36 $S_6$ , 25 $S_4$	1120	1123	30 $S_6$ , 23 $S_4$ , 19 $S_1$
	4	1173	1161	31 $S_5$ , 22 $S_1$ , 19 $S_4$	1013	1016	55 $S_5$ , 15 $S_2$ , 13 $S_6$
	5	798	801	73 $S_1$ , 15 $S_6$	719	722	55 $S_1$ , 19 $S_6$ , 12 $S_4$
	6	368	382	59 $S_4$ , 16 $S_1$ , 11 $S_5$	287	298	57 $S_4$ , 14 $S_5$ , 13 $S_6$
$A_{2g}$	7	1338		67 $S_8$ , 33 $S_7$	1058		66 $S_8$ , 34 $S_7$
	8	1052		66 $S_7$ , 34 $S_8$	745		64 $S_7$ , 36 $S_8$
$E_g$	9	2939	2935	69 $S_{11}$ , 26 $S_{10}$	2177	2203	59 $S_{11}$ , 36 $S_{10}$
	10	2877	2877	65 $S_{10}$ , 26 $S_{11}$	2096	2113	57 $S_{10}$ , 35 $S_{11}$
	11	1455	1450	26 $S_{14}$ , 20 $S_{11}$ , 25 $S_{12}$	1220	1213	46 $S_9$ , 13 $S_{12}$ , 12 $S_{13}$
	12	1347	1347	37 $S_{13}$ , 22 $S_9$ , 12 $S_{16}$	1077	1074	25 $S_{14}$ , 23 $S_{16}$ , 21 $S_{12}$
	13	1259	1270	23 $S_{13}$ , 17 $S_{15}$ , 20 $S_{16}$	928	940	38 $S_{13}$ , 21 $S_{16}$ , 24 $S_9$
	14	1040	1032	63 $S_9$ , 18 $S_{15}$	796	801	47 $S_9$ , 19 $S_{15}$ , 14 $S_{16}$
	15	785	786	27 $S_9$ , 20 $S_{16}$ , 19 $S_4$	634	635	18 $S_9$ , 20 $S_{16}$ , 16 $S_{14}$
	16	434	427	49 $S_{12}$ , 27 $S_9$ , 12 $S_{14}$	378	375	42 $S_{12}$ , 20 $S_9$ , 20 $S_{14}$
	$A_{1u}$	17	1338		56 $S_{18}$ , 37 $S_{17}$	1206	
18		1114		68 $S_{17}$ , 17 $S_{19}$ , 15 $S_{18}$	870		57 $S_{17}$ , 40 $S_{18}$
19		1101		51 $S_{17}$ , 37 $S_{19}$ , 12 $S_{18}$	783		60 $S_{19}$ , 35 $S_{17}$
$A_{2u}$	20	2945	2933	59 $S_{21}$ , 38 $S_{20}$	2186	2206	40 $S_{20}$ , 55 $S_{21}$
	21	2884	2862	59 $S_{21}$ , 38 $S_{20}$	2099	2111	48 $S_{20}$ , 47 $S_{21}$
	22	1467	1457	36 $S_{24}$ , 36 $S_{23}$ , 26 $S_{22}$	1107	1092	33 $S_{23}$ , 32 $S_{22}$ , 25 $S_{24}$
	23	1042	1039	40 $S_{22}$ , 35 $S_{24}$ , 13 $S_{23}$	908	917	49 $S_{24}$ , 20 $S_{22}$ , 15 $S_{21}$
	24	521	520	44 $S_{22}$ , 30 $S_{23}$ , 22 $S_{24}$	392	394	35 $S_{23}$ , 36 $S_{22}$ , 25 $S_{24}$
$E_u$	25	2942	2933	81 $S_{27}$ , 11 $S_{26}$	2174	2206	64 $S_{27}$ , 27 $S_{26}$
	26	2868	2862	79 $S_{26}$ , 11 $S_{27}$	2099	2111	62 $S_{26}$ , 29 $S_{27}$
	27	1455	1457	25 $S_{31}$ , 25 $S_{29}$ , 21 $S_{28}$	1161	1164	29 $S_{25}$ , 16 $S_{28}$ , 19 $S_{31}$
	28	1360	1346	39 $S_{32}$ , 20 $S_{25}$ , 19 $S_{30}$	1072	1070	21 $S_{31}$ , 20 $S_{32}$ , 21 $S_{28}$
	29	1259	1260	29 $S_{29}$ , 15 $S_{28}$ , 14 $S_{30}$	984	991	43 $S_{28}$ , 15 $S_{32}$ , 16 $S_{25}$
	30	903	906	20 $S_{25}$ , 24 $S_{30}$ , 16 $S_{32}$	715	720	52 $S_{25}$ , 17 $S_{31}$ , 9 $S_{32}$
	31	861	863	70 $S_{25}$ , 16 $S_{31}$	682	687	33 $S_{30}$ , 21 $S_{31}$ , 19 $S_{32}$
	32	228	241	52 $S_{28}$ , 34 $S_{25}$	183		50 $S_{28}$ , 33 $S_{25}$

<sup>a</sup>Root-mean-square error = 8.3 <sup>b</sup>Root-mean-square error = 12.4.

Table VI. Symmetry Coordinates for Cyclohexane,  $C_{2h}$ 

$A_g$	$S_1 = R_1 + R_3 + R_4 + R_6$	$S_8 = \gamma_1 + \gamma_4$	
	$S_2 = R_2 + R_5$	$S_9 = \alpha_1 + \alpha_6 + \alpha_7 + \alpha_{12}$	
	$S_3 = a_2 + a_3 + a_5 + a_6$	$S_{10} = \alpha_2 + \alpha_5 + \alpha_8 + \alpha_{11}$	
	$S_4 = a_1 + a_4$	$S_{11} = \alpha_3 + \alpha_4 + \alpha_9 + \alpha_{10}$	
	$S_5 = e_2 + e_3 + e_5 + e_6$	$S_{12} = \epsilon_1 + \epsilon_6 + \epsilon_1 + \epsilon_{12}$	
	$S_6 = e_1 + e_4$	$S_{13} = \epsilon_2 + \epsilon_5 + \epsilon_8 + \epsilon_{11}$	
	$S_7 = \gamma_2 + \gamma_3 + \gamma_5 + \gamma_6$	$S_{14} = \epsilon_3 + \epsilon_4 + \epsilon_9 + \epsilon_{10}$	
$B_g$	$S_{15} = R_1 - R_3 + R_4 - R_6$	$S_{20} = \alpha_2 - \alpha_5 + \alpha_8 - \alpha_{11}$	
	$S_{16} = a_2 - a_3 + a_5 - a_6$	$S_{21} = \alpha_3 - \alpha_4 + \alpha_9 - \alpha_{10}$	
	$S_{17} = e_2 - e_3 + e_5 - e_6$	$S_{22} = \epsilon_1 - \epsilon_6 + \epsilon_7 - \epsilon_{12}$	
	$S_{18} = \gamma_2 - \gamma_3 + \gamma_5 - \gamma_6$	$S_{23} = \epsilon_2 - \epsilon_5 + \epsilon_8 - \epsilon_{11}$	
	$S_{19} = \alpha_1 - \alpha_6 + \alpha_7 - \alpha_{12}$	$S_{24} = \epsilon_3 - \epsilon_4 + \epsilon_9 - \epsilon_{10}$	
	$A_u$	$S_{25} = R_1 + R_3 - R_4 - R_6$	$S_{31} = \alpha_2 + \alpha_5 - \alpha_8 - \alpha_{11}$
		$S_{26} = R_2 - R_5$	$S_{32} = \alpha_3 + \alpha_4 - \alpha_9 - \alpha_{10}$
$S_{27} = a_2 + a_3 - a_5 - a_6$		$S_{33} = \epsilon_1 + \epsilon_6 - \epsilon_7 - \epsilon_{12}$	
$S_{28} = e_2 + e_3 - e_5 - e_6$		$S_{34} = \epsilon_2 + \epsilon_5 - \epsilon_8 - \epsilon_{11}$	
$S_{29} = \gamma_2 + \gamma_3 - \gamma_5 - \gamma_6$		$S_{35} = \epsilon_3 + \epsilon_4 - \epsilon_9 - \epsilon_{10}$	
$S_{30} = \alpha_1 + \alpha_6 - \alpha_7 - \alpha_{12}$			
$B_u$		$S_{36} = R_1 - R_3 - R_4 + R_6$	$S_{43} = \alpha_1 - \alpha_6 - \alpha_7 + \alpha_{12}$
	$S_{37} = a_2 - a_3 - a_5 + a_6$	$S_{44} = \alpha_2 - \alpha_5 - \alpha_8 + \alpha_{11}$	
	$S_{38} = a_1 - a_4$	$S_{45} = \alpha_3 - \alpha_4 - \alpha_9 + \alpha_{10}$	
	$S_{39} = e_2 - e_3 - e_5 + e_6$	$S_{46} = \epsilon_1 - \epsilon_7 - \epsilon_7 + \epsilon_{12}$	
	$S_{40} = e_1 - e_4$	$S_{47} = \epsilon_2 - \epsilon_5 - \epsilon_8 + \epsilon_{11}$	
	$S_{41} = \gamma_2 - \gamma_3 - \gamma_5 + \gamma_6$	$S_{48} = \epsilon_3 - \epsilon_4 - \epsilon_9 + \epsilon_{10}$	
	$S_{42} = \gamma_1 - \gamma_4$		

Table XIII. This is a severe test of the dipole moment derivatives since errors in the latter are magnified when they are squared to give the calculated intensities, and since errors in the L matrix also will appear in the calculated intensities. The calculated intensities are in rather good agreement with the observed intensities. The ratio of the calculated intensities for the  $d_{11}$  compound is the same as that of the observed intensities (1.35). It may be concluded that the dipole moment derivatives given in Table XI are appropriate for cyclohexane.

The symmetry coordinates for the  $A_{2u}$  modes and the corresponding induced dipoles are given in Figure 7. As has been found for all hydrocarbons except acetylene, the signs of the  $\partial\mu/\partial S$  for

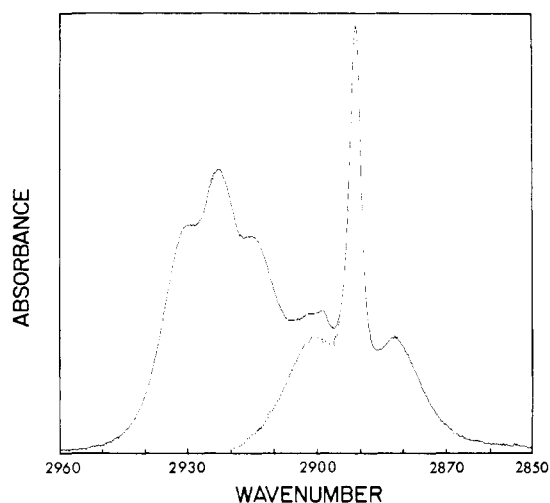


Figure 6. The C-H stretching region of cyclohexane- $d_{11}$  (pressure broadened,  $0.24\text{-cm}^{-1}$  resolution).

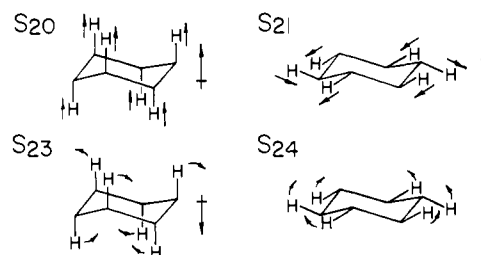


Figure 7. Symmetry coordinates and induced dipoles for the  $A_{2u}$  modes of cyclohexane.

the C-H stretching modes correspond to a bond dipole  $\text{C}^+-\text{H}^-$ , and this is the direction of the moment obtained by direct integration of the wave functions.<sup>5</sup> In the case of acetylene, integration

**Table VII.** Calculated Frequencies for  $C_{2h}$  Cyclohexanes ( $\text{cm}^{-1}$ )

		cyclohexane- $d_4^a$		cyclohexane- $d_8^b$	
		calcd	obsd	calcd	obsd
$A_g$	1	2945	2928	2941	2924
	2	2874	2850	2876	2850
	3	2177	2162	2178	2160
	4	2101	2102	2104	2112
	5	1465	1454	1459	1448
	6	1349	1341	1232	1233
	7	1260	1263	1120	1113
	8	1142	1127	1063	1051
	9	1072	1068	943	953
	10	1029	1022	800	798
	11	780	782	763	767
	12	673	675	699	702
	13	411	416	414	413
	14	331	342	307	319
$B_g$	15	2939	2904	2177	2190
	16	2876	2878	2097	2095
	17	1454	1439	1325	
	18	1333		1229	
	19	1215	1209	1160	1144
	20	1157	1157	1053	
	21	865	863	911	905
	22	835	840	786	
	23	776		639	642
	24	426	416	383	381
$A_u$	25	2942	2935	2174	2208
	26	2868	2863	2100	2116
	27	1455	1459	1322	1322
	28	1322	1323	1273	
	29	1256	1254	1164	
	30	1155	1150	1076	1068
	31	1032	1031	926	927
	32	990	998	900	
	33	786	794	744	749
	34	741	749	723	
	35	224		186	
	$B_u$	36	2941	2927	2940
37		2882	2863	2876	2862
38		2177	2194	2181	2195
39		2100	2105	2100	2105
40		1463	1455	1459	1453
41		1358	1355	1156	1159
42		1241	1245	1115	1103
43		1090	1084	1048	1050
44		1001	1012	949	953
45		846		743	728
46		799	802	723	
47		474	476	431	433
48		198		206	

<sup>a</sup>Root-mean-square error = 8.7 <sup>b</sup>Root-mean-square error = 10.7.

**Table VIII.** Scaling Factors for Force Constants in Internal Coordinates<sup>a</sup>

mode	calcd	SF	adj.
C-C stretch	4.940	0.902	4.456
a C-H stretch	5.463	0.838	4.575
e C-H stretch	5.556	0.855	4.749
a C-C-H bend	1.629	0.800	1.305
e C-C-H bend	1.632	0.799	1.307
C-C-C bend	2.825	0.862	2.437

<sup>a</sup>The off-diagonal scaling factors were taken as the geometrical mean of the corresponding diagonal scaling factors. The force constants are given in  $\text{mdyn}/\text{\AA}$ .

gave  $C-H^+$  which again corresponds to the sign of the dipole moment derivative.

The C-C-H bending modes lead to signs for  $\partial\mu/\partial S$  corresponding to the apparent motion of a relatively positively charged hydrogen. We have shown that this results from limited orbital following with the hydrogen moving ahead of the electrons in the bonding region.<sup>5</sup>

A more detailed analysis of the force field and dipole moment derivatives will be postponed until we have completed a corre-

**Table IX.** Force Constants in Terms of Symmetry Coordinates<sup>a</sup>

	1	2	3	4	5	6		
1	4.525	0.179	0.046	0.581	0.358	0.470		
2		4.572	0.081	-0.136	0.054	-0.232		
3			4.783	-0.079	-0.240	-0.058		
4				2.793	1.184	0.978		
5					2.090	1.131		
6						2.009		
	7	8						
7	0.537	0.037						
8		0.617						
	9	10	11	12	13	14	15	16
9	4.177	0.040	0.109	0.400	0.435	0.019	0.371	-0.049
10		4.576	0.040	-0.157	-0.016	-0.077	-0.113	-0.192
11			4.731	-0.167	-0.114	-0.191	-0.055	-0.057
12				1.792	0.446	0.854	0.607	0.728
13					1.073	0.534	0.265	0.507
14						1.522	0.510	0.902
15							0.924	0.551
16								1.680
	17	18	19					
17	3.966	0.447	0.338					
18		0.766	-0.018					
19			0.576					
	20	21	22	23	24			
20	4.626	0.020	-0.123	-0.066	-0.193			
21		4.729	-0.255	-0.238	-0.058			
22			1.809	1.010	0.826			
23				1.841	1.225			
24					2.042			
	25	26	27	28	29	30	31	32
25	4.931	0.233	0.097	1.474	0.471	0.146	0.340	-0.141
26		4.550	0.067	-0.019	0.033	-0.048	-0.221	-0.127
27			4.760	-0.115	-0.201	-0.098	-0.057	-0.047
28				3.216	0.948	0.722	0.823	0.272
29					1.722	0.569	0.837	0.507
30						0.888	0.485	0.313
31							1.621	0.561
32								0.991

<sup>a</sup> Units:  $\text{mdyn}/\text{\AA}$ .

**Table X.** Infrared Band Intensities

freq range, $\text{cm}^{-1}$	$A$ , $\text{km}/\text{mol}$	% error <sup>a</sup>	
a. Cyclohexane- $d_0$			
3100-2890	20, 25	283	2.5
2890-2600	21, 26	82.6	3.2
1495-1426	22, 27	20.6	1.5
1376-1326	28	0.11	b
1303-1217	29	2.88	1.8
1082-1017	23	1.41	2.4
958-888	30	2.26	1.9
888-807	31	3.23	2.0
554-496	24	0.45	b
b. Cyclohexane- $d_{12}$			
2500-2152	20, 25	121	1.6
2152-1950	21, 26	84.1	1.7
1198-1130	27	4.85	1.2
1130-1042	22, 28	5.27	1.1
1042-952	29	5.01	1.0
952-874	23	3.15	0.9
774-702	30	1.10	1.7
702-642	31	1.74	1.2

<sup>a</sup>Percent error in the slope (i.e., in  $A$ ). <sup>b</sup>The band was too weak to allow a meaningful estimate of the error.

sponding analysis of the spectrum of cyclobutane. Cyclohexane and cyclobutane have similar geometries with axial and equatorial hydrogens, and can be described by using the same types of internal and symmetry coordinates. Thus, this pair of molecules

**Table XI.** Dipole Moment Derivatives with Respect to Symmetry Coordinates ( $D/(\text{\AA} \text{amu}^{1/2})$ )

	mode	$d_0$	$d_{12}$	av
$A_{2u}$	20	-1.70	-1.85	$-1.78 \pm 0.08$
	21	0.74	0.60	$0.67 \pm 0.07$
	22	0.47	0.48	$0.47 \pm 0.01$
	23	0.44	0.38	$0.41 \pm 0.03$
	24	0.88	0.87	$0.87 \pm 0.01$
$E_u$	25	-0.38	-0.39	$-0.39 \pm 0.01$
	26	-0.46	-0.52	$-0.49 \pm 0.03$
	27	-1.52	-1.60	$-1.56 \pm 0.04$
	28	0.17	0.22	$0.19 \pm 0.02$
	29	0.46	0.55	$0.49 \pm 0.06$
	30	0.24	0.30	$0.27 \pm 0.03$
	31	0.01	0.10	$0.05 \pm 0.05$
	32	0.10	0.15	$0.12 \pm 0.03$

**Table XII.** Experimental Polar Tensors<sup>a</sup>

atom	$d_0$			$d_{12}$		
	x	y	z	x	y	z
1x	0.416	0.000	-0.302	0.407	0.000	-0.241
1y	0.000	0.193	0.000	0.000	0.192	0.000
1z	0.166	0.000	0.600	0.152	0.000	0.640
7x	-0.818	0.000	0.359	-0.846	0.000	0.302
7y	0.000	0.060	0.000	0.000	0.052	0.000
7z	0.317	0.000	0.100	0.375	0.000	0.118
13x	0.167	0.000	0.071	0.207	0.000	0.053
13y	0.000	-0.019	0.000	0.000	-0.010	0.000
13z	-0.271	0.000	-0.699	-0.314	0.000	-0.759
Average Values						
	x	y	z			
1x	$0.412 \pm 0.005$	0.000	$-0.272 \pm 0.031$			
1y	0.000	$0.193 \pm 0.001$	0.000			
1z	$0.159 \pm 0.007$	0.000	$0.620 \pm 0.020$			
7x	$-0.833 \pm 0.013$	0.000	$0.330 \pm 0.029$			
7y	0.000	$0.056 \pm 0.004$	0.000			
7z	$0.346 \pm 0.028$	0.000	$0.109 \pm 0.009$			
13x	$0.187 \pm 0.022$	0.000	$0.062 \pm 0.009$			
13y	0.000	$-0.015 \pm 0.002$	0.000			
13z	$-0.293 \pm 0.021$	0.000	$-0.729 \pm 0.030$			

<sup>a</sup>The numbering of the atoms and the coordinate system are shown in Table II. Units:  $D/\text{\AA}$ .

should be ideal for studying the effect of structural change on both bond strengths and charge distributions.

### Experimental Section

**Spectra.** The gas-phase Raman spectra were obtained with a Spex Ramalog spectrometer with a  $2\text{-cm}^{-1}$  band-pass, a  $4\text{-cm}^3$  multipass gas cell fitted with elliptical Brewster windows, and the  $4880\text{-nm}$  line of an

**Table XIII.** Calculated and Observed Infrared Intensities ( $\text{km/mol}$ )

mode	$d_0$		$d_{12}$		
	calcd	obsd	calcd	obsd	
$A_{2u}$	20	106	109	60.7	59.7
	21	54.2	44.4	23.3	28.3
	22	12.8	13.5	4.7	4.4
	23	1.4	1.4	3.3	3.2
	24	0.5	0.5	0.3	0.4 <sup>a</sup>
$E_u$	25	182	174	60.0	61.3
	26	43.2	38.2	50.6	55.7
	27	6.4	4.4	4.1	4.9
	28	0.1	0.1	0.4	0.8
	29	2.6	2.9	4.6	5.0
	30	2.4	2.3	1.2	1.1
	31	3.2	3.2	1.7	1.7
	32	0.0	0.0 <sup>a</sup>	0.0	0.0 <sup>a</sup>
Cyclohexane- $d_{11}$					
		calcd	obsd		
equatorial H		37.8	36.4		
axial H		27.9	27.0		
ratio		1.35	1.35		

<sup>a</sup>Estimated values.

Argon-ion laser operating at 700 mW. Signal averaging was carried out with 100 scans. The infrared spectra were determined with a Nicolet 7199 FTIR spectrometer. An instrument resolution of  $0.06\text{ cm}^{-1}$  was used for observing the band contours and locating the band origins, whereas a resolution of  $0.24\text{ cm}^{-1}$  was used for the integrated intensity measurements of the pressure broadened spectra. A pressure cell of the type described by Dickson et al.<sup>18</sup> with a path length of 72.5 mm was used for the intensity measurements. The sample pressures were measured with Wallace and Tiernan absolute pressure gauges. Integrations were carried out by using the software supplied with the spectrometer. The integrals were converted to  $\text{km torr cm/mol}$  by multiplying by  $2.303RT$  or  $1.43617T$ .

**Calculations.** The force field was calculated with the program GAM-ESS<sup>19</sup> with use of the standard 4-31G basis set.<sup>7</sup> The normal coordinate calculations were carried out with modified versions of the programs of Schachtschneider.<sup>20</sup> The conversion of intensities to dipole moment derivatives made use of the signs of the calculated dipole moment derivatives and programs written by R. C. Dempsey.<sup>21</sup>

**Compounds.** Cyclohexane was Aldrich 99+%, cyclohexane- $d_{12}$  was Aldrich 99.5%, and cyclohexane- $d_{11}$  was obtained from Merck and Co/Isotopes (98%).

**Acknowledgment.** This investigation was supported by National Science Foundation grant CHE-83-18955.

**Registry No.** Cyclohexane, 110-82-7; cyclohexane- $d_{12}$ , 1735-17-7.

**Supplementary Material Available:** A list of force constants for internal coordinates (5 pages). Ordering information is given on any current masthead page.